R&D Activities on Photovoltaics at CNEA - Argentina

Juan Plá[1,2], Mariana Tamasi[1,2], Mariela Videla[1], Analía Moreno[1,2], Ismael Eyras[1], Martha Díaz Salazar[1,2], Claudio Bolzi[1], José Olima[1], Juan I. Pérez[1], Nadia Kondratiuk[1,2], Julio Durán[1] and Mónica Martínez Bogado[1,2]

[1] Departamento Energía Solar – CAC-CNEA, San Martín, Provincia de Buenos Aires (Argentina)

[2] Instituto de Nanociencia y Nanotecnología – CONICET-CNEA, San Martín, Provincia de Buenos Aires (Argentina)

Abstract

The Solar Energy Department (DES) of the National Atomic Energy Commission (CNEA) has been developing R&D photovoltaic (PV) activities from several decades, addressed both to space and terrestrial applications. These activities include the development of device characterization techniques, design, simulation, testing and integration of solar panels for space applications, development and fabrication of PV radiometers for solar radiation characterization, and the instrumentation of PV systems for distributed generation applications. In this work, various particular issues are reviewed, focused on devices and systems devoted to the solar resource evaluation and energy generation. After a brief introduction of the DES historical research lines, latest results on solar sensors and PV systems projects are presented.

Keywords: PV sensors, solar radiation, radiometers, PV module characterization, distributed generation

1. Introduction

PV solar energy became the principal alternative for the transition to greenhouse gas emissions (GHG) free world in order to mitigate the rise in global temperatures caused by climate change. Almost all countries signed the Paris Agreement in 2015, and implemented consequent policies to reduce the GHG. Within this framework, in all scenarios PV emerges as the main power technology (IEA, 2022).

The growth in installed solar PV capacity, resulting from promotion and investment policies implemented by many countries in recent decades, is shown in Figure 1. The milestone of 1 TW of cumulative installed capacity was reached in 2022, while in 2024 this capacity more than doubled, reaching 2.2 TW. However, this remarkable growth is not enough to limit the global temperature increase to 1.5°C, as established in the Paris Agreement, for which it is necessary to multiply this value several times (Haegel et al, 2023; Jäger-Waldau, 2025). According to the updated scenario developed by the IEA (International Energy Agency) leading to net zero emissions (NZE) in 2050, renewable sources should account for 59% of the energy generated in 2030 and over 88% in 2050, for total values of 23,337 TWh and 70,936 TWh, respectively (Jäger-Waldau, 2025). The forecast for solar PV generation in particular is 9,212 TWh in 2030, for a total of 6.7 TW installed (Jäger-Waldau, 2025), i.e., three times the 2024 figure.

Argentina has participated in this general trend, and since 2006 has introduced various national legislative initiatives aimed to promote renewable energy, as have several provincial states. These policy decisions facilitated the adoption of renewable energy generation technologies, including solar PV. Although there is a strong predominance of thermal power plants based on fossil fuels, there is also a sustained growth of renewable sources, including wind, solar, and hydroelectric power, the latter with capacities of up to 50 MW (hydroelectric power plants with a capacity greater than 50 MW are considered separately by the Law 27,191 of promotion of renewables). As a result, the total generation from renewable sources in 2024 was 22,877 GWh, 17.2% (3,941 GWh) of which came from solar PV (CAMMESA, 2025).

The total power of PV plants in operation as of May 2025 amounted to 2,177 MW, mainly installed in the

10.18086/swc.2025.03.62 Available at http://proceedings.ises.org

northwest of the country (854 MW) and in the Cuyo region (835 MW). Distributed generation from renewable sources has made some progress, albeit still in its infancy: as of June 2025 there were 2,918 user-generators registered in the country, with a total installed capacity of approximately 78 MW (MECON, 2025).

The Solar Energy Department of the Argentinean CNEA has early been developing R&D activities on PV from the end of 80's. These included, as example, basic and applied research on Si and III-V devices (Bruno et al., 1999; Barrera et al., 2008; Socolovsky et al., 2015), on orbit experiments (Bolzi et al., 2002), radiation test development facility (Ibarra et al., 2019), radiation damage experiments (Alurralde et al., 2004; Ochoa et al., 2017) and design, testing, and integration of solar panels for satellites (Alurralde et al., 2013).

More recently, the Department has focused on new activities related to energy generation. These activities can be divided into two issues: the development and fabrication of PV radiation sensors and radiometers, and the execution of PV system projects and associated research. The following sections focus on these latter topics.

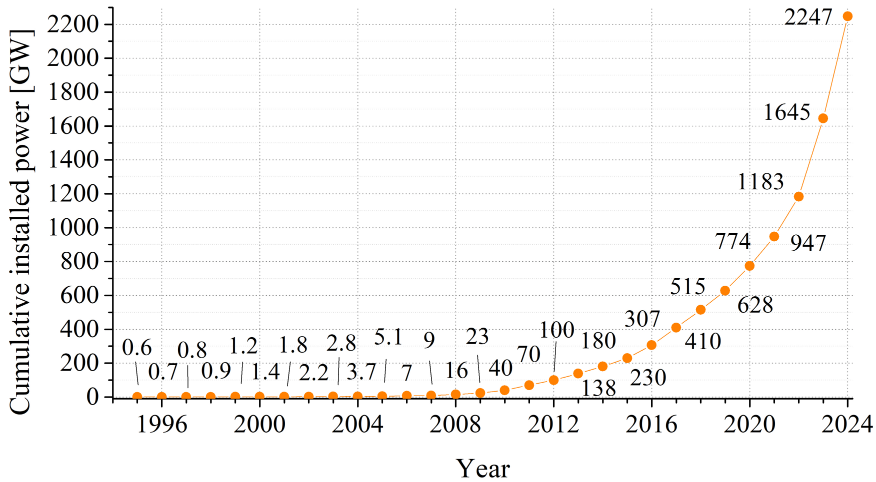

Figure 1: Evolution of global installed photovoltaic solar power capacity (1995-2024). Based on data extracted from REN21 (2013), REN21 (2024), and IEA (2025).

2. Photovoltaic sensors and radiometers

The Solar Energy Department (DES) of the CNEA has a long-standing tradition in the development and fabrication of silicon photovoltaic (PV) sensors, with activities initiated in 1998. These devices leverage the Department's core expertise in PV cell technology, utilizing crystalline silicon p-n junctions fabricated on Czochralski-grown wafers. The fabrication process involves a modified one-step diffusion of phosphorus and aluminum, creating an n^+pp^+ structure, followed by photolithography and the deposition of Ti-Pd-Ag metal contacts (Martínez Bogado et al., 2015; Bolzi et al., 2013). This robust and reproducible process allows for the customization of sensors for a wide range of applications, both terrestrial and spatial, by tailoring key variables such as the short circuit current and spectral response.

A significant achievement has been the adaptation of its spectral response for specific measurement purposes. For instance, to develop a sensor for ultraviolet (UV) radiation, the front junction diffusion process was modified. This initiative addresses the critical need for affordable and accessible instrumentation to monitor solar UV radiation, which is known to cause adverse health effects such as neoplasms, mutations, photoaging, immunosuppression, and cataracts.

The development strategy takes a dual approach: integrating commercial optical components for rapid prototyping, and in-house fabricating custom thin film filters to enhance performance and contribute to technological sovereignty.

An initial UV radiometer prototype has been successfully fabricated, integrated, and deployed. This instrument is based on a custom-fabricated silicon photovoltaic sensor, the spectral response of which was specifically modified to enhance its sensitivity in the UV region. This was achieved by optimizing the front junction diffusion process to create a shallower junction, resulting in a significant increase in spectral response (e.g., a 67% enhancement at 340 nm) (Kondratiuk et al., 2016). The sensor is coupled with a commercial UV band-pass filter to selectively target the desired spectral band (e.g., UVA or UVB). The prototype is equipped with a custom-designed transimpedance amplifier to condition the low-level output signal.

This prototype has been installed on the rooftop of the TANDAR building at the Constituyentes Atomic Center, co-located with the DES solar resource assessment station, which includes both commercial and in-house developed instrumentation (see Figure 2). This setup enables for direct comparison and validation. Since its installation, data collection has been ongoing, and the acquisition system has been fine-tuned. Preliminary data analysis involves studying the correlation between the measurements from the DES prototype and a calibrated commercial UV radiometer.

In parallel, a significant research effort is dedicated to the design and fabrication of custom thin-film optical filters. This work aims to create high-performance, tailored filters that are integrated to the sensor package, moving beyond reliance on commercial components. The fabrication process involves depositing multilayer stacks of silicon oxide and silver onto quartz substrates and directly onto silicon sensors using sputtering deposition techniques.

The deposited thin films have been characterized by measuring their spectral reflectance and transmittance. The experimental results show good agreement with simulated performance, demonstrating the successful fabrication of filters with high transmittance in the target UV region and strong blocking of unwanted portions of the solar spectrum. The characterization of complete sensor devices integrated with these multilayer filters is currently in progress. This advancement represents a crucial step towards achieving a fully national, state-of-the-art UV radiometer with optimized spectral selectivity.

These developments in UV radiometry demonstrate the Department's ability to adapt its core PV technology to overcome specific measurement challenges. This contributes to environmental monitoring and public health by providing locally developed, low-cost alternatives to imported instruments.

Figure 2: Left, DES UV radiometer and commercial Kipp & Zonen UV radiometer. Right, global radiation (G) radiometer.

Furthermore, research has been conducted on designing and simulating thin-film optical filters (metal-dielectric multilayers) to be coupled with these sensors, enabling the creation of customized radiometers for specific UV bands (UVA or UVB) by blocking unwanted portions of the solar spectrum (Videla et al., 2020).

For other terrestrial applications, the PV sensors are encapsulated into cylindrical bases with a ground glass diffuser to improve the angular response and protect the device. In this configuration, a global radiation (G) radiometer is obtained (Figure 2). These instruments provide a low-cost alternative to thermopile-based pyranometers, offering advantages such as high response speed and national/regional availability (see Videla et al. 2020).

Additionally, using the same configuration as the instruments described in the previous paragraph but including an optical filter, radiometers that measure the portion of the solar spectrum between 400 and 700 nm were developed. These instruments measure Photosynthetically Active Radiation (PAR) and target the spectral interval that plants use for photosynthesis.

The G and PAR radiometers developed at the DES represent a mature and consolidated technological solution that is currently in the commercialization phase (TRL 8/9) and are used by various university research groups and scientific centers in Argentina and other Latin American countries (Honduras, Bolivia, Guatemala). This high level of maturity has been validated through rigorous performance studies. A comprehensive study was conducted to evaluate the performance of a DES-developed PV radiometer against a commercial First-Class (ISO 9060:2018 Class B) thermopile pyranometer. Both sensors, installed in the plane-of-array (POA) at a 34° tilt, recorded data over twelve months. The analysis of hourly and daily irradiation integrals showed a stable performance of the PV sensor. While instantaneous differences existed, the daily integrals showed a mean percentage difference of -4.17% with a standard deviation of ±1.78% (Videla et al., 2020), demonstrating accuracy more than sufficient for solar resource assessment and energy yield prediction in photovoltaic systems.

Crucially, when data from both sensors was used to simulate the energy yield of an 85 kW grid-connected PV system, the results showed a high degree of concordance. The annual energy yield difference was only 2%, which is within the simulation software's typical uncertainty margin (~3%). Differences in monthly energy yield were generally below 4%, demonstrating the PV radiometer's suitability for assessing the energy yield of PV systems, where integrated daily values are the primary input. (Videla et al., 2020).

Prototypes for other specialized applications have also been developed, such as a submersible radiometer for aquatic environments and a sensor for agronomic use measuring the Normalized Difference Vegetation Index (NDVI; Figure 3). The NDVI sensor development required a specific design to achieve the necessary spectral selectivity. The NDVI is calculated from the reflectance in two distinct spectral bands: the Red (R) region around 660 nm and the Near-Infrared (NIR) region around 850 nm, using the formula NDVI = (NIR - R) / (NIR + R). To create a dedicated NDVI radiometer, a prototype was designed and constructed featuring an aluminum base housing four custom silicon PV sensors. Two sensors face upwards to measure incident solar radiation, and two face downwards to measure the radiation reflected by the target surface (e.g., a crop canopy). For each pair (up and down), one sensor is dedicated to the Red band and the other to the NIR band. This four-sensor configuration allows for the direct calculation of reflectances in each band, which are the inputs for the NDVI formula.

Spectral selection is achieved using commercial band-pass filters centered at 630 nm (Red) and 800 nm (NIR), each with a 10 nm bandwidth, whose transmittance curves were characterized to ensure they met the required specifications. The signal levels from the filtered sensors are low (on the order of 0.1-0.15 mA for I_{SC} under sunlight), requiring the use of sensors with a large active area (75.5 mm²) to maximize the short circuit current, limited only by the diameter of the available filters.

Field measurements were conducted on different grass samples to validate the prototype. The calculated NDVI values showed repeatability across different days and varying irradiance conditions, and the results correlated well with the observed health and density of the grass samples, with NDVI values ranging from ~0.2 for sparse vegetation to ~0.97 for dense, healthy turf. This low-cost, portable instrument provides a valuable tool for precision agriculture, allowing for non-destructive, in-situ monitoring of plant health, biomass, and nitrogen uptake directly in the field, supporting decision-making for local producers (Moreno, 2022).

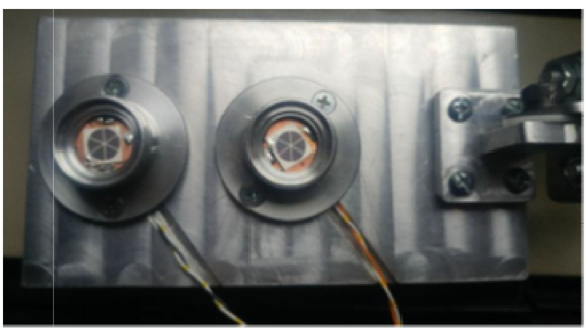

Figure 3: Aluminum base with NDVI instrument.

3. Photovoltaic systems

An institutional investment project is being executed to align CNEA with the current laws that regulate and promote renewable energies in the country. The project will also contribute to Argentina's international commitments on environmental issues. Alongside this main objective, R&D activities are being conducted within this framework.

Part of these activities focused on building-integrated photovoltaic systems (BIPV), as the presented in the pictures of Figure 4. Beyond the integration into the building structure available, the influence of the PV installation on the building indoor environment is also a matter of study. For this purpose, a system is being designed to continuously cover a large part of a flat roof. This system will have an East-West (E-W) structure and will include appropriate temperature and humidity sensors. The project aims to collect robust data based on monthly averages.

Figure 4: BIPV installations. A semitransparent pergola (left), and one forming the eaves of the building (right).

3.1. Energy monitoring and simulation

Other subjects under study are the expected and real energy generation, together with energy pay-back time (EPBT) calculation. The EPBT for a particular 50 kW terrace-mounted system, based on monocrystalline PERC Si modules and a concrete counterbalanced structure, is presented elsewhere (González Bisciglia et al., 2023).

Monitoring the energy generated is important for evaluating the contribution of the PV systems installed to meeting the energy consumption needs of the CNEA buildings, while also allowing estimate the efficiency of these systems and can give early warnings to be issued for possible failures.

As an example of this task, Figure 5 shows the monthly generation of one of the installations, corresponding to a 20 kW system for the months of January to July 2025.

The monitoring of the energy generated was carried out using data provided by the inverter of the installation, while the simulation was performed using the PVSyst program (PVSyst, 2025) based on global solar radiation data on a horizontal plane recorded near the site.

With regard to the differences between generation and simulation observed, the distances between rows of PV modules were reviewed in the simulation, and those shadows produced by the surrounding building structure were also included. The differences between measured and simulated generation observed in the months around the winter solstice (May, June, and July) would seem to indicate that the shadow losses obtained by simulation do not fully correspond to reality. It is therefore necessary to review the location and height of the adjacent (or nearby) buildings, as well as the unevenness of the roof, in order to detect the possible origin of the differences identified. Another possible source of these differences, to be explored, is the possible mismatch between the configuration of the module strings and those actually installed, as well as in the internal modeling of the module assumed by PVSyst. By the way, solar radiation is monitored with a pyranometer located at an adjacent building, and it is eventually affected by the shadow of the TANDAR heavy ions accelerator facility tower (see Figure 6): this could explain the difference appeared in January. In any case, the field of view of the pyranometer could be different, and for instance the quantification of the albedo may introduce some error. All of these are lessons learned in order to get a reliable tool for energy prediction.

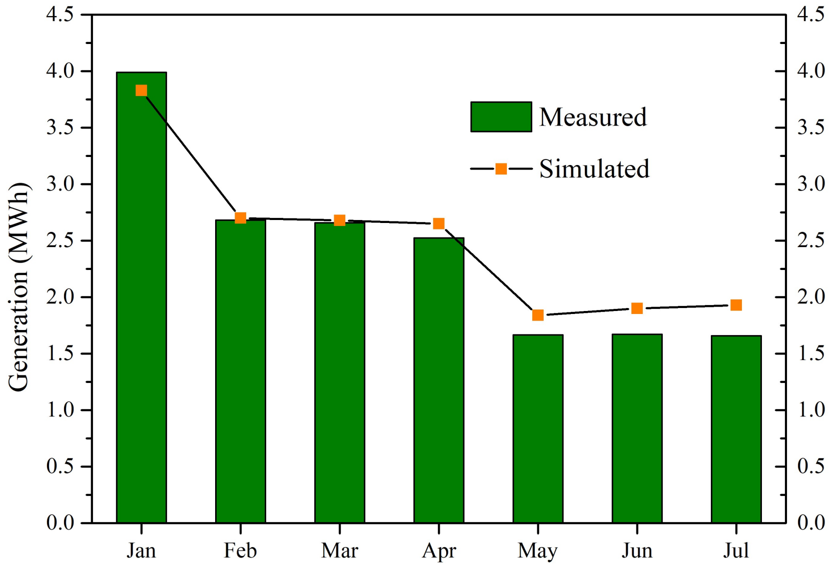

Figure 5: Monthly generation between January and July 2025 of a 20 kW system. The line represents the energy obtained by simulation using the PVSyst program.

Figure 6: View of the radiometers bench under the shadow of TANDAR accelerator tower. Approximate location of the 20 kW system is indicated.

3.2. Module characterization

Module characterization procedures based on current IEC standards were developed in order to assess the health of system components at the reception stage, in the frame of particular events as strong storms, as well as their time evolution under operation. Particularly, current-voltage curve under standard conditions and electroluminescence (EL) are nowadays available. Results of I-V measurements and EL images comparing a reference unused module and a module from the same batch affected by an extreme meteorological event are presented as follows.

To measure the current-voltage (I-V) electrical characteristic, an Alpha-Omega Large Area Pulsed Solar Simulator (LAPSS) and a calibrated Solar World reference cell were used. The measurement was performed at room temperature (21 ± 1 °C) and an irradiance of 1 kW m^{-2}.

On December 17, 2023, an extreme weather event occurred in the region of the city of Buenos Aires and its surroundings. As a consequence, part of one 50 kW PV installation sited at CNEA suffered severe damages (see Figure 7). This 50 kW system is divided in two wings (east and west, because of their relative orientations; Figure 6), sited at two different roof levels with, respectively, 68 and 48 modules Amerisolar of 445 W.

While the east wing suffered minor damages, the west wing was majorly affected. This is due to a significant influence on wind speed from the topography of the module installation site for the west wing, located near the CNEA's TANDAR heavy ion accelerator tower, verified through calculations using CFD (Computational Fluid Dynamics) to simulate real conditions based on the Navier-Stokes equations. Particularly, the wind speed coming from the SW direction is significantly increased by the topography of the site: In this case (west wing), the CFD analysis indicates the formation of a wake that begins shortly before the crest of the TANDAR tower and extends toward the region where the modules were located. As a result, the increase in speed has a maximum of 37%.

Figure 7: Left: partial view of the 50 kW PV system; on the back of the image, the TANDAR accelerator tower, on the right, the west wing (48 modules). Right: status of the west wing after the storm occurred on 17 December, 2023. South-West direction is indicated.

The module characterization procedures were applied to the 22 modules that passed a coarse visual inspection, i.e. with no major structural damage. An unused module of the same model, taken as reference, was also characterized.

Some examples of the measured I-V curves are showed in Figure 8. All curves were corrected to the standard temperature (25 ºC); the modules were identified as '0' to '22', being '0' the reference one. Table 1 presents the percentage deviation of the electrical parameters extracted from the corrected curves with respect to those of the reference module.

The percentage deviations of each parameter P from the corresponding values of the reference module (P_0) were then calculated using the following expression:

$$\Delta P = 100 \times \frac{P - P_0}{P_0} \qquad \text{(eq. 1)}$$

The values obtained for P_{MAX} (maximum power), V_{OC} (open circuit voltage), I_{SC} (short circuit current) and FF (fill factor) for selected cases are shown in Table 1. The trend observed, particularly in the deviation average, is that basically all the electrical parameters of the modules tested show lower values (i.e., negative percentage differences) with respect to those corresponding to the reference module, with P_{MAX} standing out with an average of -4.3%.

The standard deviations of the averages are relatively high, especially in the case of P_{MAX} and FF (see Table 1), which is due to the specific cases of modules where degradation above (or well above) the average is verified. Using a percentage deviation of P_{MAX} greater than 4% as an exclusion criterion (which excludes modules 6, 11, 12, 20, and 22 from the average calculation), the parameters maintain the same trend but with a lower (and below the average) standard deviation with the exception of FF where, excluding the most severe cases, the average remains essentially unchanged. This can be seen in the quantities identified with (*) in Table 1. The percentage deviation of P_{MAX} used as an exclusion criterion is based on the fact that this parameter shows a clear degradation compared to the reference module, and in particular is consistent with the tolerance declared by the manufacturer for P_{MAX} (±3%). As a result, although apparently in good shape, all the modules tested showed degradation respect the reference one.

Table 1: Percentage deviations in the electrical parameters of selected modules tested under standard conditions, relative to those of the reference module. Deviations average calculated on all the modules tested is included, as well as the deviation average subtracting the worse cases.

Module	ΔP_{MAX}	ΔV_{OC}	ΔI_{SC}	ΔFF
6	-9.3	-0.5	-3.5	-5.6
11	-27.4	-2.3	-8.1	-19.1
12	-4.2	-0.7	-1.3	-2.3
20	-4.5	-0.1	-1.7	-2.7
22	-9.2	-1.2	-4.0	-4.3
Average (22 modules)	-4.3	-0.8	-2.2	-1.4
Standard deviation	5.5	0.6	1.6	4.2
Average* (17 modules)	-2.5	-0.8	-1.7	0.1
Standard deviation*	0.9	0.6	0.8	0.6

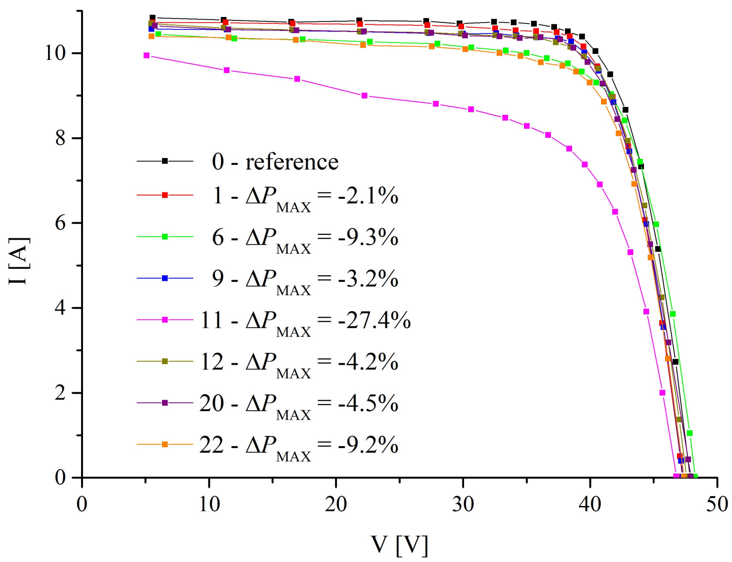

Figure 8: Examples of the I-V measured curves. In the inset, the corresponding values for P_{MAX} degradation respect to the reference module.

Electroluminescence tests at 100% of I_{SC} were performed on the same I-V tested 22 modules, as well as on the reference module. EL images of the selected (worse) cases, modules 6, 11, 12, 20, and 22, are showed in Figure 9. A first observation is that in all cases there are widespread defects in a large number of cells, ranging from multiple breaks in the most extreme cases (modules 6, 11, and 22) to cracks that run across the width from side to side. In isolated cases, cells with little or no emission are also observed, indicative of poor electronic, and therefore, electrical performance. In general terms, there is a correlation between the number of cells with defects and the degradation of P_{MAX}, which is (see Table 1) for module 6, -9.3%, module 11, -27.4%, module 12, -4.2%, module 20, -4.5%, and module 22, -9.2%.

From the EL test performed resulted that 11 modules (including the particular and worse cases analyzed) presented cracks at least in some cells, while the other 11 remaining showed defects similar to the reference module. Notwithstanding this, it is reported that after an accelerated aging test, small cracks (not side to side or defining pieces of cells) can evolve to more severe damage (Köntges et al., 2011), but this topic is beyond of the scope of this work.

The results of module characterization showed that the effects of severe storms on this component of a system under operation can be catastrophic, although modules appear to be healthy. A deep inside provided by the combination of I-V and EL tests established a correct evaluation of the real status.

The problem consequence of the extreme meteorological event put also the attention on the support structure utilized, composed by concrete counterweights and 2 clamps holding 2 modules at once by the short side. This configuration admits oscillations due to the dynamical charge of wind and in the case of a strong gust, when one module loosens, the same thing happens with the adjacent one, causing a domino effect. This is in part the situation observed in Figure 7.

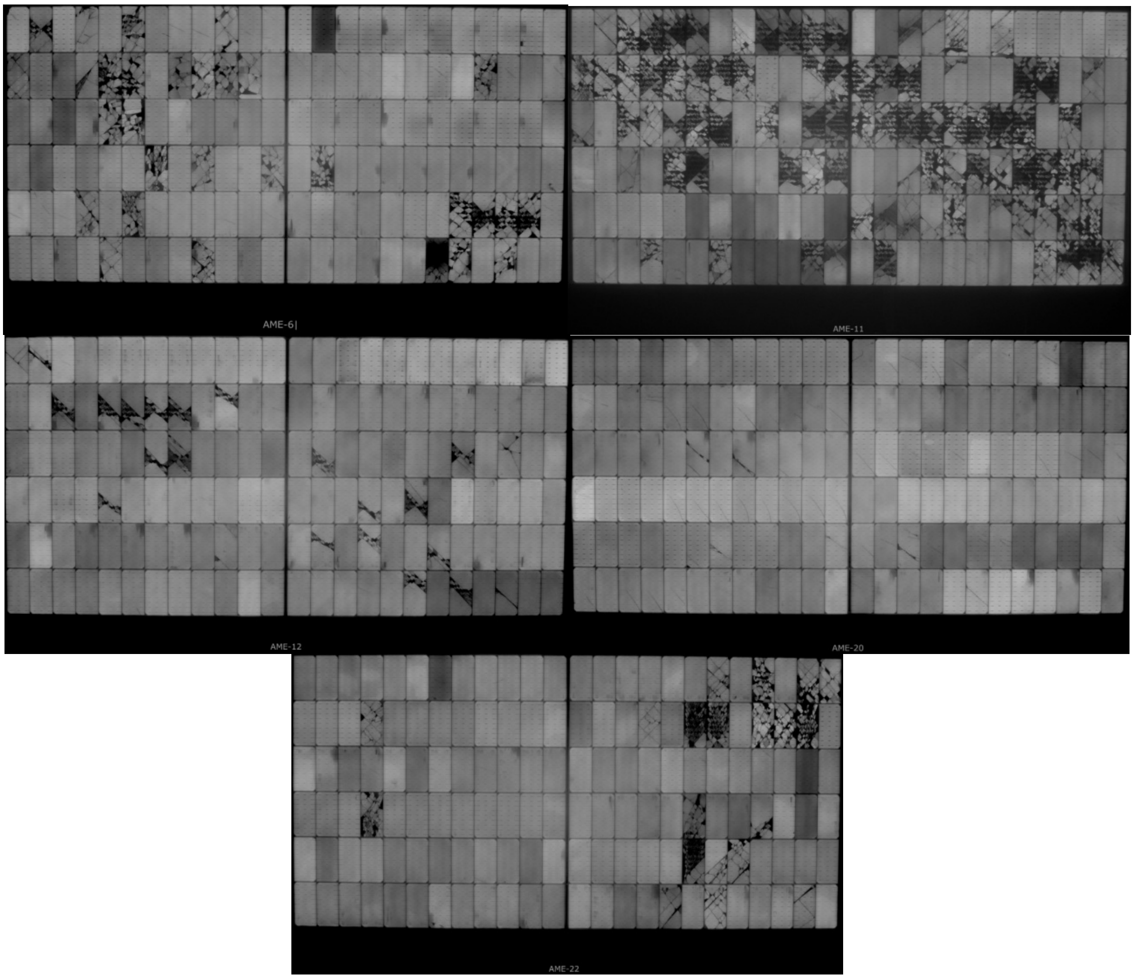

Figure 9: Electroluminescence images of selected modules for currents set at 100% of I_{SC} (see text). From left to right and top to bottom, the images correspond to modules 6, 11, 12, 20, and 22.

4. Conclusions

The accumulated expertise in designing and fabricating silicon photovoltaic devices at DES-CNEA has been effectively leveraged to create a new generation of reliable, low-cost terrestrial sensing instruments. The domestically developed low-cost global radiation PV radiometer performs similarly to commercial instruments, and achieves an excellent cosine response with a relative percentage error below 10% even at high elevation angles. This radiometer has been successfully commercialized at a local and regional level.

The development of ultraviolet radiometers at DES-CNEA demonstrates the successful adaptation of silicon photovoltaic technology for specialized environmental monitoring. The prototype, deployed alongside reference instrumentation, has enabled preliminary validation and continuous technical refinement, particularly in signal conditioning. Parallel progress in custom thin-film filter fabrication promises enhanced spectral selectivity and technological sovereignty. These advancements establish a foundation for producing reliable, cost-effective UV monitoring solutions with significant potential applications in public health and environmental science.

Furthermore, the promising initial prototype development of the spectrally selective NDVI sensor demonstrates significant potential for adapting these instruments to precision agriculture. This provides local producers and research institutions with a reliable, readily available, and cost-effective tool for monitoring solar resource utilization, crop development, and ecosystem functioning, thereby reducing dependency on imported commercial devices. These technological advancements significantly enhance national capabilities in the field of solar radiometric measurements.

The experience gained in R&D activities at CNEA in distributed generation using grid tied PV systems has led to a series of lessons learned, which are summarized below.

On the one hand, it is necessary to correctly evaluate the structures and counterweights, taking into account the particular topography of the PV installation site and its influence on the mechanical load caused by the wind. In particular, it is advisable to use fasteners on the long sides of PV modules in cases where the modules are more than 2 m long, which is the dominant trend in the market. The appearance of cracks in PV modules may be due to significant oscillations of the modules in the presence of even light winds, as a result of inappropriate fastening systems.

Likewise, the evaluation and monitoring of the energy generated by PV installations through comparisons with simulations allows for the early detection of faults, the definition of cleaning needs, and the analysis of losses due to shadows, which in some cases can be avoided with an appropriate design. A correct evaluation of solar radiation and the possible effects of shadows caused from adjacent structures results mandatory. Further hypotheses that could imply errors in the system simulation, such as non-actual wiring of the strings and an incorrect electrical model of the module, are currently being verified.

It is also considered advisable to define procedures for the acceptance of PV modules through electrical testing and electroluminescence observation in order to detect parameters that are out of range.

In summary, the R&D activities on PV applications at the National Atomic Energy Commission (CNEA) in Argentina were reviewed. Both consolidated developments and more recent research were included, with a focus on lessons learned for knowledge appropriation.

5. Acknowledgments

The authors would like to thank Sebastián Muñoz, Javier Fernández Vázquez, Marcelo Ramírez, Carlos Rinaldi, Alejandro Krautner, Oscar Romanelli, Agustín Marconi, and Juan N. Cox for their collaboration and contributions to this work. The authors would also like to thank the AeroMat Group from the Materials Department of the CNEA, in particular its director Lucio Ponzoni, for the CFD calculations.

6. References

Alurralde, M., et al., 2004. Experimental and theoretical radiation damage studies on crystalline silicon solar cells. Sol. Energ. Mat. Sol. Cells. 82, 531-542. https://doi.org/10.1016/j.solmat.2003.11.029

Alurralde, M., et al., 2013. Development of solar arrays for argentine satellite missions. Aerosp. Sci. Technol. 26, 38-52. https://doi.org/10.1016/j.ast.2012.02.012

Barrera, M., Plá, J., Bocchi, C., Migliori, A., 2008. Antireflecting-passivating dielectric films on crystalline silicon solar cells for space applications. Sol. Energ. Mat. Sol. Cells. 92, 1115-1122. https://doi.org/10.1016/j.solmat.2008.03.021

Bolzi, C.G., Bruno, C.J., Durán, J.C., Godfrin, E.M., Martínez Bogado, M.G., Merino, L.M., Plá, J.C., Tamasi, M.J.L., Barrera, M., 2002. First experiment of argentine solar cells in space: modules fabrication, characterisation, and telemetry data analysis from SAC-A satellite. Sol. Energ. Mat. Sol. Cells. 73, 269-280. https://doi.org/10.1016/S0927-0248(01)00137-4

Bolzi, C., Martínez Bogado, M.G., Tamasi, M.J.L, 2013. Reseña del Desarrollo de Sensores Solares en CNEA para Misiones Satelitales. Energías Renovables y Medio Ambiente. 31, 29 – 36. https://portalderevistas.unsa.edu.ar/index.php/erma/article/view/1488/1438 [accessed 23 October 2025]

Bruno, C.J., Martínez Bogado, M.G., Plá, J.C., Durán, J.C., 1999. Determination of the minority carrier lifetime in solar cells: a novel biased OCVD technique. Phys. Status Solidi A. 174, 231-238. https://doi.org/10.1002/(SICI)1521-396X(199907)174:1<3C231::AID-PSSA231>3E3.0.CO;2-8

CAMMESA (2025). Informe Anual 2024. Mercado Eléctrico Mayorista. Compañía Administradora del Mercado Mayorista Eléctrico [2024 Annual Report. Wholesale Electricity Market. Wholesale Electricity Market Management Company; in Spanish]. https://cammesaweb.cammesa.com/informes-y-estadisticas/ [accessed 22 October 2025]

Durán, J.C., Eyras, I., Plá, J., Videla, M., Krautner, A., Bolzi, C.G., Pérez, J.I., Martínez Bogado, M., 2024. Advances in investment projects for distributed electrical generation with photovoltaic systems at CNEA. Acta de la Reunión de Trabajo de la ASADES. 11, 126-137. http://asades.org.ar/wp-content/uploads/2025/03/ACTAS-2024.pdf [accessed 14 May 2025]

González Bisciglia, L., Videla, M.E., Pedace, R., 2023. Energy payback time of a distributed photovoltaic generation system in Argentina. Energías Renovables y Medio Ambiente. 52, 16-24. https://portalderevistas.unsa.edu.ar/index.php/erma/article/view/4364 [accessed 14 May 2025]

Haegel, N.M., et al., 2023. Photovoltaics at multi-terawatt scale: Waiting is not an option. Science 380, 6640, 39-42. https://doi.org/10.1126/science.adf6957

Ibarra, M.L., Garcia, J.A., Dato, A., Yaccuzzi, E., Prario, I., Filevich, A., Barrera, M., Alurralde, M., 2019. E.D.R.A., the Argentine facility to simulate radiation damage in space. Radiat. Phys. Chem. 154, 79–84. https://doi.org/10.1016/j.radphyschem.2018.08.032

IEA, 2022. World Energy Outlook 2022. International Energy Agency, Paris. October 2022. https://www.iea.org/reports/world-energy-outlook-2022 [accessed 14 May 2025]

IEA, 2025. Snapshot of Global PV Markets 2025. International Energy Agency - Photovoltaic Power Systems Programme. April 2025. https://iea-pvps.org/snapshot-reports/snapshot-2025/ [accessed 22 October 2025]

Jäger-Waldau, A., 2025. Snapshot of photovoltaics - March 2025. EPJ Photovolt. 16, 22. https://doi.org/10.1051/epjpv/2025012

Kondratiuk, N.Y., Tamasi, M.J.L., Martínez Bogado, M.G., 2020. Modificación de la respuesta espectral de un dispositivo fotovoltaico para su utilización como sensor de radiación ultravioleta. Energías Renovables y Medio Ambiente. 37, 77–84. https://portalderevistas.unsa.edu.ar/index.php/erma/article/view/1382 [accessed 23 October 2025]

Köntges M., Kunze, I., Kajari-Schröder, S., Breitenmoser, X., Bjørneklett, B., 2011. The risk of power loss in crystalline silicon based photovoltaic modules due to micro-cracks. Sol. Energ. Mat. Sol. Cells. 95, 1131–1137. https://doi.org/10.1016/j.solmat.2010.10.034

Martínez Bogado, M., Tamasi, M., Bolzi, C., Raggio, D., 2015. Desarrollo de sensores solares en Argentina, aplicaciones terrestres y espaciales. Revista Brasileira de Energia Solar. 6, 57-67. https://doi.org/10.59627/rbens.2015v6i1.128

MECON (2025). Generación Distribuida en Argentina. Reporte Anual 2024. Ministerio de Economía [Distributed Generation in Argentina. Annual Report 2024. Ministry of Economy; in Spanish]. https://www.argentina.gob.ar/sites/default/files/reporte_anual_2024.pdf [accessed 22 October 2025]

Moreno, A., 2022. Ph.D. Thesis, Desarrollo y fabricación de sensores fotovoltaicos de radiación: aplicaciones espaciales y radiómetros de espectro selectivo [Development and fabrication of photovoltaic radiation sensors: space applications and selective spectrum radiometers]. Universidad Nacional de San Martín, Argentina.

Ochoa, M., et al., 2017. 10 MeV proton irradiation effects on GaInP/GaAs/Ge concentrator solar cells and their component subcells. Sol. Energ. Mat. Sol. Cells. 159, 576-582. https://doi.org/10.1016/j.solmat.2016.09.042

PVSyst, 2025. PVSyst - Photovoltaic Software. https://www.pvsyst.com/en/ [accessed 22 October 2025]

Socolovsky, H., Yaccuzzi, E., Plá, J., 2015. Spectral and dynamical study of III-V triple junction solar cells and the application to multiflash I-V measurement. Prog. Photovolt.: Res. Appl. 23, 1330-1339. http://dx.doi.org/10.1002/pip.2569

Videla, M.E., Martínez Bogado, M., Tamasi, M., Moreno, A., Kondratiuk, N., Díaz Salazar, M., 2020. Comparison between a commercial class B pyranometer and a photovoltaic radiometer developed in the Solar Energy Department. Energías Renovables y Medio Ambiente. 46, 43-48. https://portalderevistas.unsa.edu.ar/index.php/erma/article/view/2841 [accessed 14 May 2025]